



Measurements of tumor size using CT and PET compared to histopathological size in non-small cell lung cancer

Funda Aydın, Levent Dertsiz, Evrim Sürer Budak, Akın Yıldız, Gülay Özbilim, Fırat Güngör

PURPOSE

In this study, we aimed to compare the tumor sizes determined by maximum morphological computed tomography (CT) and functional positron emission tomography (PET) with the histopathological size to determine which method provides the best correlation with the histopathological size in lung carcinoma patients.

MATERIALS AND METHODS

Forty lung carcinoma patients (39 males, one female) diagnosed histopathologically from surgical resection materials were included in this retrospective study. The mean age (\pm standard deviation, SD) of the patients was 67.8 ± 10.3 years with a range of 44 to 81 years. The PET scans were performed within the same week as the CT scan. In the CT scans, the morphological tumor sizes were measured three-dimensionally by the longest transaxial section in the parenchymal and mediastinal screening window. The functional tumor sizes were also measured three-dimensionally in the PET scans. These two measurement values were compared with the histopathological size using Bland-Altman plotting. Bland-Altman plotting was also performed to define the 95% limits of agreement, which was presented as the bias ± 1.96 SD.

RESULTS

The histopathological sizes were measured in a range of 1.2 to 7.5 cm. The maximum measurement of the tumors on the CT scans showed a lower concordance (mean difference, -0.30) than that obtained from PET, and the SD was found to be larger than the PET (1.96 SD was 3.50 for CT and 2.50 for PET).

CONCLUSION

The PET measurements of tumor size were more compatible with the histopathological sizes than the CT measurements in patients with non-small cell lung cancer.

Lung cancer is the leading cause of cancer death in most industrialized countries (1). Non-small cell lung carcinoma (NSCLC) accounts for 85% of all cases of lung cancer, with small cell lung cancer and mesothelioma comprising the other 15% (1).

Patients with early stage disease who undergo complete resection sometimes experience recurrence, and the reported five-year survival rates after surgery, even in stage I lung cancer, range from 60% to 77% (1–3).

Surgery is the current standard of care for patients with stage I NSCLC, but it can be associated with significant morbidity and even mortality, particularly because patients suffering from lung cancer are often elderly with high comorbidity rates (4).

Radical radiotherapy (RT) is the most commonly used treatment modality for NSCLC (5). The single most important component of planning radical, potentially curative RT involves an assessment of the tumor size. Unnecessary toxicity in the surrounding tissue may occur if the tumor size is overestimated, and underestimation may result in part of the tumor receiving an inadequate radiation dose, leading to treatment failure (5).

Fluorine-18-fluorodeoxyglucose positron emission tomography (^{18}F -FDG PET) has become increasingly important in the diagnosis of lung cancer. ^{18}F -FDG PET allows differentiation between malignant and benign lesions based on differences in glucose metabolism between normal and cancer tissues (6). Previous studies have demonstrated that ^{18}F -FDG PET is more accurate than computed tomography (CT) for the diagnosis and staging of NSCLC (7, 8). The main disadvantage of ^{18}F -FDG PET is the poor quality of the anatomic information. To overcome this limitation, new imaging systems using integrated ^{18}F -FDG PET-CT have been recently developed (9). The use of ^{18}F -FDG PET with the addition of CT since the development of PET-CT devices has increased for staging NSCLC (10). PET-CT has become an important technique for the initial diagnosis, staging, and therapeutic follow-up in lung cancer (11).

In addition, the use of ^{18}F -FDG PET-CT in RT treatment planning for the definition of gross tumor volume has similarly increased and continues to gain popularity (12). Manual contouring of the tumor boundaries on CT images is still the conventional methodology for target volume definition. On the other hand, and despite a high spatial resolution, the delineation on CT alone may be biased by insufficient contrast between the tumor and healthy tissues (e.g., in cases of atelectasis, pleural effusion, and fibrosis or tumors attached to the chest wall or mediastinum). Several studies have investigated the impact of delineation performed on fused ^{18}F -FDG PET-CT images and have found significant modifications of the treatment plan (size, location, or shape of the gross tumor volume) (13) and reduced inter- and intraobserver variability (14, 15).

From the Departments of Nuclear Medicine (FA, ✉ afunda@akdeniz.edu.tr, E.S.B., A.Y., F.G.), Thoracic Surgery (L.D.), and Pathology (G.Ö.), Akdeniz University School of Medicine, Antalya, Turkey.

Received 13 September 2012; revision requested 17 September 2012; revision received 5 November 2012; accepted 11 November 2012

Published online 9 January 2013
DOI 10.5152/dir.2013.053

Several recent studies have investigated the correlation between tumor histopathology (HP) measurements and the threshold of FDG uptake (14, 16). Previous studies investigating NSCLC tumor delineation on PET-CT images have hypothesized that the use of these methods has a significant influence on the determination of the anatomic or metabolic lesion size and the heterogeneity of the activity distribution (17). However, in the literature there is only one study investigating whether PET or CT images more accurately measure the histopathologic size of metabolically active tumors (18).

In this study, we aimed to compare NSCLC tumor dimensions measured using preoperative PET and CT scans with the actual tumor measurements obtained following surgical resection, retrospectively.

Materials and methods

Patients

This study was designed as a retrospective clinical study. Forty patients with confirmed NSCLC (39 males and one female; age range, 44–81 years; mean age, 67.8±10.3 years; 1 cm or more in diameter by CT and a maximum standardized uptake value [SUV_{max}] of 2.5 or more by PET) were included between June 2008 and July 2011. The collection of impact data and outcomes was approved by our institutional ethics committee. All patients underwent an ^{18}F -FDG PET-CT examination for staging purposes before treatment. ^{18}F -FDG PET-CT imaging was performed according to EANM guidelines (19). We excluded hyperglycemic patients (plasma glucose level higher than 120 mg/dL), patients who underwent neoadjuvant chemoradiotherapy before curative resection, and patients with tumors with a low-affinity for ^{18}F -FDG and tumors

measuring less than 1 cm in size. All patients were asked to avoid strenuous exercise for 24 hours before PET-CT. The patients were instructed to fast for a minimum of six hours before the examination. Free-breathing PET and CT images were acquired 45–60 min after injection of 360±20 MBq ^{18}F -FDG. An oral contrast agent was used for CT examination, and intravenous contrast material was not given. All patients were confirmed to be normoglycemic, and no plasma glucose correction was planned. A total of seven 3-min bed positions with overlap were used for whole-body PET (Biograph-16 True Point PET-CT, Siemens Healthcare, Erlangen, Germany) acquisitions, which were corrected for attenuation using the CT data (no breath-hold; section thickness, 6 mm; pitch, 1.5; 120 mAs; 130 kVp) and iteratively reconstructed using the ordered-subset expectation maximization algorithm (three iterations, 21 subsets).

Within one week after the PET-CT examinations, all patients underwent surgery (36 lobectomies, one segmentectomy, one pneumonectomy, and two wedge resections), which allowed further macroscopic examination. All specimens were processed in the same way. Namely, the fresh specimens were placed on ice, and one pathologist measured the maximum diameter of the tumor in three dimensions (14). Specimen shrinkage, estimated at approximately 10%, was not considered because the measurements were performed before fixation in formalin, allowing for subsequent immunohistochemical examination, for which the biopsy specimens were paraffin-embedded.

PET and CT tumor delineation

The PET-CT images were evaluated using a Syngo fusion platform (Siemens Healthcare) by two nuclear medicine

physicians. One of them is also a radiologist. They had five years of experience in PET-CT interpretation and were unaware of the clinical and pathologic results. In this study, CT and ^{18}F -FDG PET imaging were evaluated in order to calculate the lesion size, and manual delineation on fused PET-CT images was not considered. Only primary tumors were delineated on both CT and PET images independently. In the case of discrepancy between the two physicians, a consensus was reached in all cases.

We used an SUV_{max} value of 2.5 as a threshold to define the tumor boundaries on the PET-CT images. All tumors were measured on the PET and CT images because the SUV_{max} value was more than 2.5 and the maximum measurement of the tumor was more than 1 cm. We excluded the tumors with SUV_{max} values lower than 2.5 and maximum measurements less than 1 cm.

The tumor anatomic sizes were manually delineated on the CT scans by two observers without knowledge of the PET information. The functional tumor volumes were manually delineated on PET images by two observers who were blinded to the CT data. The CT and PET images were presented as separate files, and these measurements were performed randomly. On the CT scans, the primary tumors were delineated using the lung and mediastinum windows setting (window width, 1200 Hounsfield unit [HU]; window center, -600 HU for lung window; window width, 300 HU; window center, 40 HU for mediastinum window). The longest diameter of the tumor on the CT (at both parenchymal and mediastinal windows) and PET scans was measured in a three-dimensional display (Fig. 1).

Statistical analysis

A statistical software (MedCalc, version 12.2.1.0, MedCalc Software



Figure 1. a–c. A 64-year-old man with non-small cell lung carcinoma. PET scan (a), CT scan obtained with a soft-tissue window (b), and CT scan obtained with a lung window (c) show the measurements of the primary lung tumor.

bvba, Mariakerke, Belgium) was used to analyze the data. To evaluate the correlation between the HP, PET, and CT (windows: soft-tissue, ST; lung, L) measurements, we used the Pearson product moment correlation coefficients after checking the assumptions. All data were expressed as the mean±standard deviation (SD). These two measurement values were compared with the HP size using Bland-Altman plotting. Bland-Altman plotting was also performed to define the 95% limit of agreement, which was presented as a bias ±1.96 SD (20). Bias, a measure of systematic error, was defined as $1/N(\sum dSIZE)$, where $dSIZE$ is the difference in SIZE (i.e., $SIZE_{HP} - SIZE_{other}$) and N is the number of cases.

Additionally, the percentage of bias (bias%) for CT and PET measurement values was calculated.

Results

Table 1 shows the maximum measured sizes of the 40 tumors based on either macroscopic examination or PET and CT. The mean ±1.96 SD tumor maximum size value was 3.96 ± 3.57 cm (range, 1.2–7.5 cm) for the HP measurements. The mean ±1.96 SD tumor maximum size values were found to be 4.23 ± 4.19 cm, 4.62 ± 4.49 cm, and 4.20 ± 3.74 cm for CT_{ST} , CT_L , and PET, respectively. Significant differences were observed among the delineations (Fig. 2). The CT_{ST} , CT_L , and PET delineations consistently overestimated the maximum sizes of all tumors. Twenty-one patients (52%) had tumors that surrounded atelectasis or pneumonia (Table 1).

All variables were significantly and positively correlated with the maximum measurement of the histologic specimen (Table 2). The highest correlation (0.88) was between PET and CT_{ST} . As a measure of the linear relationship, the high values of the correlation coefficients indicate that the linear relationships were strongly significant.

The Bland-Altman plots of agreement showed that the biases (mean difference values) were small than the difference between the maximum measurements of the tumor on HP and on PET and CT. However, the SD values in the CT and PET scans were large. According to this method, the maximum

Table 1. Summary of the patients, and comparison of tumor size on PET-CT with histopathology

Patient number	Age (years)	Tumor	HP (cm)	PET (cm)	CT_{ST} (cm)	CT_L (cm)	SUV _{max}	A or P
1	77	SCC	3.0	2.6	4.9	4.5	29.7	(+)
2	58	SCC	1.5	3.7	4.2	4.3	9.4	(+)
3	63	SCC	4.5	4.5	4.0	4.3	18.0	(-)
4	53	SCC	3.5	3.1	2.8	4.0	13.6	(+)
5	44	SCC	3.5	4.5	7.8	8.7	10.8	(+)
6	81	SCC	2.5	4.8	4.4	4.6	23.3	(-)
7	71	SCC	4.6	7.8	9.6	6.5	21.0	(+)
8	74	SCC	5.0	4.8	6.0	8.0	10.0	(+)
9	72	SCC	4.5	5.5	6.0	6.1	10.0	(-)
10	81	SCC	4.0	2.6	2.6	2.7	2.5	(-)
11	60	SCC	4.5	3.2	3.6	3.6	11.5	(+)
12	64	SCC	3.5	4.0	3.1	3.0	22.2	(-)
13	68	SCC	7.5	9.0	8.3	7.9	24.9	(-)
14	78	SCC	1.4	1.8	1.5	2.0	6.3	(-)
15	73	SCC	6.0	5.9	6.0	6.2	11.5	(+)
16	78	SCC	3.7	4.2	4.0	4.8	4.8	(+)
17	70	SCC	2.2	2.3	2.5	3.5	12.3	(+)
18	54	SCC	3.0	3.9	4.0	3.5	18.1	(+)
19	57	SCC	1.3	1.2	1.0	1.1	8.0	(-)
20	80	SCC	5.0	6.6	7.9	7.4	28.5	(-)
21	75	SCC	4.0	4.0	2.7	3.1	16.0	(-)
22	79	SCC	6.0	4.8	5.0	5.0	27.8	(-)
23	57	Adenocarcinoma	2.0	2.5	2.2	2.3	13.1	(-)
24	73	Adenocarcinoma	3.0	5.3	4.0	4.6	16.7	(-)
25	81	Adenocarcinoma	3.5	4.4	5.0	5.1	30.7	(-)
26	78	Adenocarcinoma	6.5	7.0	7.0	9.5	23.7	(+)
27	53	Adenocarcinoma	1.6	1.8	1.8	2.3	7.7	(+)
28	61	Adenocarcinoma	1.5	1.5	2.0	2.2	3.3	(+)
29	59	Adenocarcinoma	2.5	2.6	2.1	2.2	14.0	(+)
30	77	Adenocarcinoma	1.7	1.9	1.7	1.5	3.3	(-)
31	66	Adeno+SCC	2.0	1.5	1.4	1.8	7.2	(-)
32	47	Adeno+SCC	7.0	6.1	5.1	7.1	15.3	(+)
33	58	Adeno+SCC	4.0	5.5	3.5	6.2	29.9	(+)
34	75	Adeno+SCC	3.0	2.0	1.5	1.6	13.6	(-)
35	85	Adeno+SCC	4.0	3.6	3.5	3.5	15.5	(-)
36	66	LCC	6.0	6.1	6.5	8.6	16.0	(+)
37	64	Sarcoma	7.5	5.3	4.5	4.9	13.9	(-)
38	69	Sarcoma	7.4	7.5	7.7	8.0	13.4	(+)
39	63	SCC	7.0	5.7	4.0	6.1	21.7	(+)
40	71	SCC	4.5	2.6	3.5	2.3	2.5	(+)

A or P: atelectasis or pneumonia; CT_L : maximum tumor size on computed tomography with lung window; CT_{ST} : maximum tumor size on computed tomography with soft-tissue window; HP: maximum tumor size on histopathology; LCC, large cell carcinoma; PET, maximum tumor size on positron emission tomography; SCC, squamous cell carcinoma; SUV_{max}: maximum standardized uptake value.

measurement of the tumor on PET scans showed the most concordance with the maximum measurements of the histologic specimens (mean difference, -0.20). The maximum measurements of the tumors on the CT scans with soft-tissue and lung windows showed a lower concordance (mean difference was -0.30 for CT_{ST} and -0.70 for CT_L) than on the PET scans, and the SD was found to be larger than that for the PET scan (1.96 SD was 3.50 for CT_{ST}, 3.13 for CT_L, and 2.50 for PET). The Bland-Altman plots are shown in Figs. 3–5 for the PET, CT_{ST}, and CT_L imaging, respectively.

The graphic data (Fig. 3) show that two tumors were outliers regarding the agreement between the maximum histological measurements and the maximum measurements on the PET scans. In one of these cases, the maximum measurement of the tumor on the PET scans was less than that of the histologic specimen; the other had a larger measurement for the histologic specimen. Fig. 2 also shows that in one patient, the maximum measurement of the tumor on PET scans was larger than the histological measurement.

In the evaluation of the agreement between the histologic size and the maximum measurement on the CT_{ST} images (Fig. 4), four tumors were found to lie outside the area of 95% concordance. In two of these cases, the maximum measurement of the tumor on the CT scans was less than that of the histologic specimen, and the others were more than the histologic specimen. The graphic data (Fig. 5) show that two tumors were outliers regarding the agreement between the maximum histological measurements and the maximum measurement obtained from CT_L imaging.

Discussion

NSCLC accounts for 75%–80% of all lung cancers and is currently the leading cause of tumor-related death (1, 2). The optimal treatment of lung cancer relies on accurate disease staging, which is based on determination of the tumor size, regional nodal involvement, and the presence of metastasis. Accurate staging of NSCLC is essential for appropriate therapy selection. Surgery remains the mainstay of efforts to cure

Table 2. Correlation between maximum measurements on histopathology, PET, and CT for 40 patients

Variable	HP	PET	CT _{ST}	CT _L
HP	1.00			
PET	0.81 (< 0.0001)	1.00		
CT _{ST}	0.68 (< 0.0001)	0.88 (< 0.0001)	1.00	0.89 (< 0.0001)
CT _L	0.73 (< 0.0001)	0.87 (< 0.0001)	0.89 (< 0.0001)	1.00

CT_L, maximum tumor size on computed tomography with lung window; CT_{ST}, maximum tumor size on computed tomography with soft-tissue window; HP, maximum tumor size on histopathology; PET, maximum tumor size on positron emission tomography. Values are correlation coefficients (r) with P values in parantheses.

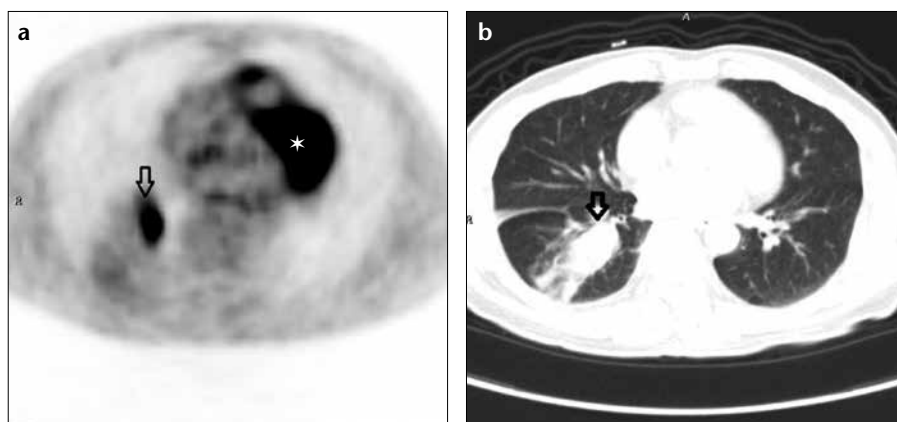


Figure 2. a, b. A 58-year-old man with non-small cell lung carcinoma. The PET scan (a) and CT scan obtained with lung window (b) show that the maximum PET and CT measurements of the primary lung tumor were larger than the histopathology measurements. The tumor maximum size as measured by PET imaging, CT with lung window, CT with soft-tissue window, and histopathology was 3.7 cm, 4.2 cm, 4.3 cm, and 1.5 cm, respectively. The figures show the hypermetabolic area in the primary tumor region with a SUV_{max} value of 9.4 (arrows), and the myocardial activity on left side (a, star).

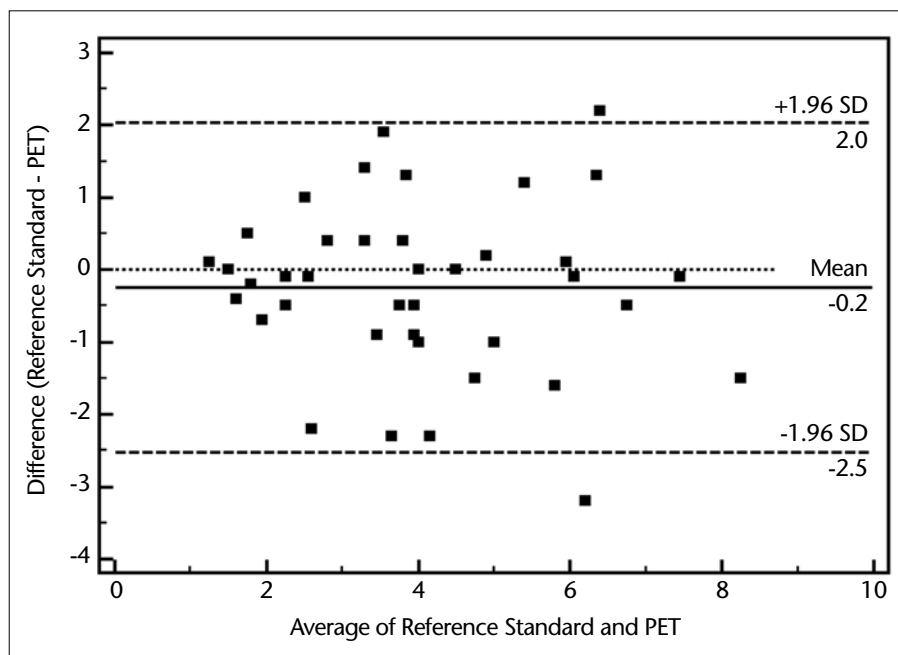


Figure 3. The Bland-Altman plot shows the agreement of the maximum measurement of the tumor in the histopathologic specimen (reference standard) and on PET imaging. Two of 40 tumors (5%) are outside the limits of agreement; the mean difference, -0.2; 95% limits of agreement, -2.5, 2.0. SD, standard deviation.

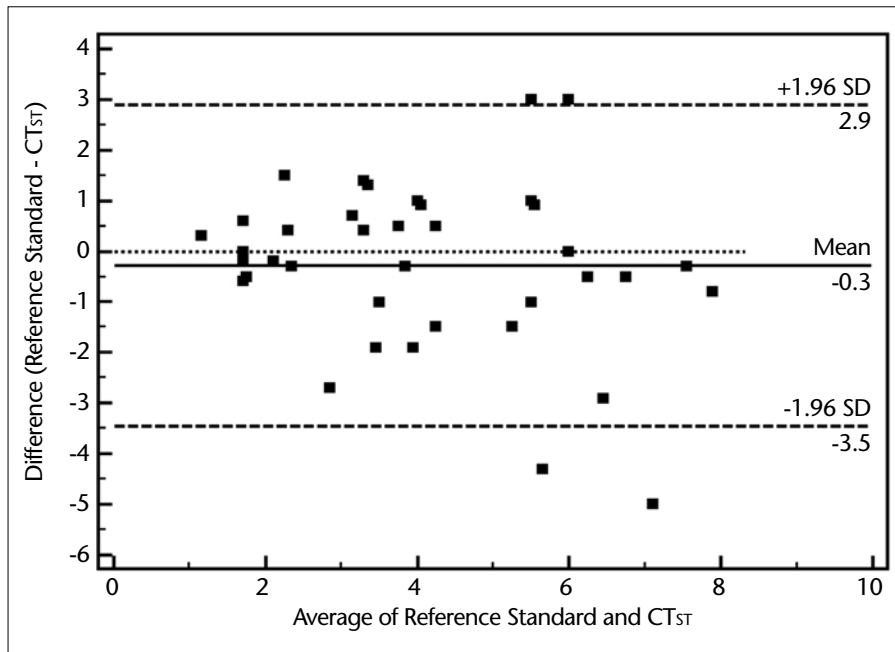


Figure 4. The Bland-Altman plot shows the agreement of the maximum measurement of the tumor in the histopathologic specimen (reference standard) and on CT_{st} imaging. Four of 40 tumors (10%) are outside limits of agreement; mean difference, -0.3; 95% limits of agreement, -3.5, 2.9. SD, standard deviation.

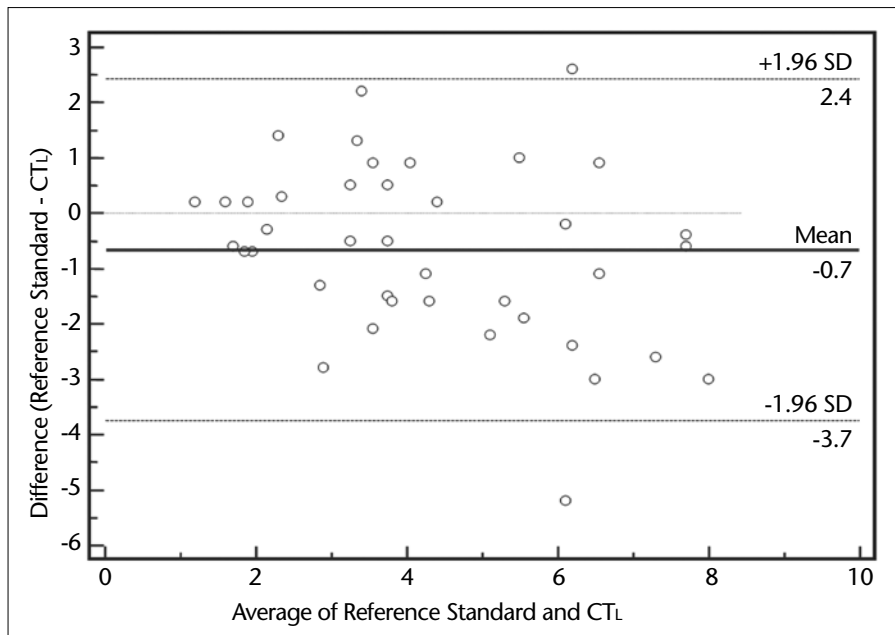


Figure 5. The Bland-Altman plot shows the agreement of the maximum measurement of the tumor in the histopathologic specimen (reference standard) and on the CT_l image. Two of 40 tumors (5%) were outside the limits of agreement; mean difference, -0.7; 95% limits of agreement, -3.7, 2.4. SD, standard deviation.

NSCLC, but the postsurgical prognosis remains poor (1, 10). Radical RT, particularly if combined with platinum-based chemotherapy, can be curative in patients with unresectable disease (21). Planning the surgical treatment or radical RT involves staging the extent of

locoregional disease in the thorax and excluding the wider metastatic disease in appropriate patients.

Although contrast-enhanced CT has been widely used for the preoperative evaluation of the tumor size and the invasion of adjacent structures, nu-

merous studies have shown that it is limited for the staging of lung cancer because of its low reliability for lymph node staging (22). Additionally, both the negative and the positive predictive values of CT for staging cancer in the mediastinum have been relatively poor in most reported series (10, 23).

PET with ¹⁸F-FDG has been reported to increase the diagnostic accuracy for the differentiation of benign and malignant lesions and to improve the identification of nodal metastasis. Functional scans obtained with FDG PET are not only complementary to those obtained with conventional modalities, but they may also be more sensitive because alterations in tissue metabolism generally precede anatomic change (24). Unlike conventional CT, PET has been shown to have a high predictive accuracy, as verified surgically, for staging the locoregional extent of lung cancer (25). The spatial resolution of PET is generally insufficient to exclude small-volume disease, and false-positive results can occur as a result of inflammatory processes. Nonetheless, PET has been shown to be substantially more accurate than CT in almost all comparative studies of the two, and there is evidence that the results of PET affect clinical decision making (25).

In this study, we retrospectively investigated the diagnostic performance of FDG PET and CT imaging for the maximum measured sizes of the tumor in NSCLC after surgery. The results showed that PET or CT alone was accurate for measuring primary lung tumors. Because the study was retrospective, volumetric measurements were not possible. Accordingly, the maximum diameter of the tumor was measured and recorded because this measurement is recorded for histologic specimens, enabling direct comparison between the histologic and imaging findings.

The highest correlation was found between the maximum measurements on PET and CT, indicating that either imaging method can be used to measure the primary tumor. Little research has been conducted to specifically investigate the radiological tumor size and how this measurement correlates with the pathological size (5). A pi-

lot study compared the gross tumor volume on CT imaging with the microscopic extent of the disease in five resected NSCLC tumors and suggested that CT overestimated the pathological size (26).

There is only one study in the literature that compares PET and CT with regard to the maximum tumor size measurement relative to the HP size (18). This study by Pawaroo et al. (18), which reported the maximum measurement of the tumor on CT scans with soft-tissue windows in NSCLC, found the highest level of concordance with the reference standard measurement of the HP. Furthermore, PET had a smaller SD, indicating less variation in the measurements. In our study, it was found that PET provided closer measurements than CT (-0.2 for PET, -0.3 for CT_{ST}, and -0.7 for CT_L). It was also established that the 1.96 SD values of the PET images were closer than those of the CT images (1.96 SD was 2.20 for PET and 3.18 for CT_{ST}, and 3.13 for CT_L).

HP measurement is regarded as the reference standard (13, 17). The maximum dimensions were used because these dimensions were used to measure the macroscopic specimens. The maximum measurements of four tumors on PET and five tumors on CT scans were almost twice those measured using macroscopic specimen because the whole lesion was not included in the contour. Although the HP type was squamous cell carcinoma, the SUV_{max} values of these tumors were high (SUV_{max} range, 9–23). However, there was a wide hypermetabolic atelectasis area surrounding the tumor in these cases.

SUV is a semiquantitative index that characterizes the tracer uptake, allowing for approximation of the glucose metabolic rate (27). The maximum SUV of primary NSCLC varies widely, with one study (17) reporting a range of 1.7–38.7. The maximum SUV is also affected by a variety of technical and biological factors (13). There is no standard method for placing contours around the tumor on PET scans, and the threshold chosen determines the tumor volume (28), which is vital in planning RT. A single maximum SUV has been found to poorly delineate the gross tumor volume and to reveal considerable variability in the volumes

obtained, especially if the tumor is heterogeneous (13, 17, 29). Hong et al. (29) performed a retrospective analysis of methods of contouring tumors with PET-CT using different SUV values. They compared the volumes obtained against the volumes obtained with CT and suggested using an SUV greater than 2.5 to differentiate between benign and malignant lesions because this value correlated best with the CT volume. This method is the one generally used (13, 29), thus we used this SUV threshold.

In our study, the SUV_{max} values of all tumors were in the range of 3.3–30.7. The maximum measurements were calculated using the PET scan because the SUV_{max} values were higher than the background. The maximum measurements of 24 tumors on PET were similar to the HP size.

In this study, the HP types of tumors included squamous cell carcinoma, adenocarcinoma, and mix type. We excluded adenocarcinoma *in situ* (AIS) (30) (except invasive adenocarcinoma) because this HP type has a lower FDG uptake on PET images than other lung tumors do (31). Higashi et al. (31) found that the mean SUV of AIS was significantly different compared to adenocarcinomas with well, moderate, and poor differentiation. These investigators concluded that glucose metabolism measured by FDG PET correlated with the degree of tumor cell differentiation for adenocarcinoma of the lung (31). In addition, AIS has been known to have a longer doubling time and a slower rate of proliferation than the other types of lung cancer (32). Therefore, it can be well understood that an AIS shows no or low FDG uptake based on the results of several studies (31, 32), and PET has been shown to miss 67% of rare tumors with a pure AIS pattern with no invasive component (33). However, in the case of an adenocarcinoma with AIS, the diagnostic performance of FDG PET was similar to that of other NSCLCs (32).

In our study, all specimens were processed in the same way; namely, the fresh specimens were put on ice, and one pathologist measured the maximum diameter of the tumor in three dimensions (14). We did not use pathologic specimens that had been preserved in

formaldehyde, which is known to cause shrinkage. Hsu et al. (33) investigated this phenomenon in the cases of 401 patients who underwent surgery for NSCLC. Those investigators compared the measurement of the pathologic specimens (>3 or <3 cm) immediately after resection and after the specimens were fixed in formaldehyde. In 40 patients (≈10%), the pathologic specimen measured less than 3 cm, but according to the surgical notes, the tumor was larger than 3 cm, changing the tumor from T2 to T1.

According to the agreement of the histologic reference standard measurement with the measurements on both soft-tissue and lung window CT scans, three tumor measurements were greater on the CT scans than in the histologic specimens. All of these patients had surrounding consolidation or collapse, indicating that CT is less accurate in these situations (Fig. 6).

The present study also had several limitations. Because the study was retrospective, volumetric measurements were not possible. The role and potential value of ¹⁸F-FDG PET scanning in the definition of target volumes have been widely investigated in recent years (34). Although the tumor volume could not be measured in this retrospective study, it was found that maximum tumor size measurements taken from PET images were close to the HP maximum size. Two widely accepted and conventional guidelines for the objective assessment of the response to therapy in patients with solid tumors include the World Health Organization (WHO) guideline, which uses bidimensional tumor measurements, and the Response Evaluation Criteria in Solid Tumors (RECIST), which uses unidimensional measurements of the longest diameter of the tumor (35). Another limitation, again related to measurement, was that although we used the maximum measurements of the tumor both in the macroscopic specimen and on the images, we did not know the plane in which the macroscopic specimen was measured. Although the macroscopic specimens were measured in three dimensions, tumor size might had been underestimated in some cases. We propose a prospective study in which specimens

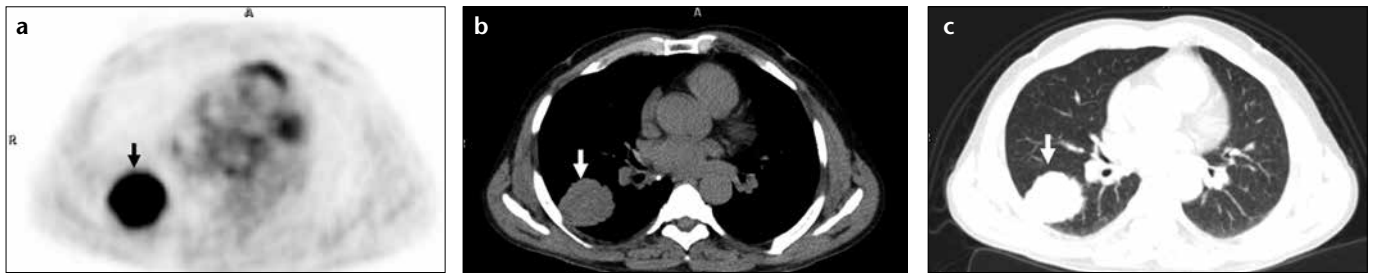


Figure 6. a–c. A 63-year-old man with lung squamous cell carcinoma. The PET scan (a) and CT scans obtained with soft-tissue (b) and lung windows (c) show that the PET and CT maximum measurements of the primary lung tumor were lower than the histopathology measurement. The tumor maximum size measured by PET scan, CT with lung window, CT with soft-tissue window, and histopathology was 5.7 cm, 6.1 cm, 4.0 cm, and 7.0 cm, respectively. The hypermetabolic area in the primary tumor region is seen by PET imaging, and the SUV_{max} is 21.7 (arrows).

are measured in a stated plane after resection. The measurement would be compared with measurements in the same plane on images. Another limitation was that tumors with SUV_{max} values lower than 2.5 and measurements less than 1 cm were excluded. The maximum measurements of all were calculated by PET scan because the SUV_{max} values were higher than the background. However, tumors with SUV_{max} values less than 2.5 cannot be calculated with PET scanning, and a measurement of less than 1 cm by CT imaging cannot be evaluated as a pathologic lesion. Because of the retrospective nature of the study, 39 males and only one female patient were included. The true population could not be reflected with these cases, but 40 patients with confirmed NSCLC were included in this study between June 2008 and July 2011. Another limitation of this study was that CT images were performed without intravenous contrast and no breath-holding. Lung tumors move during respiration, and this motion can cause volumetric deformation of the tumor image in CT scans (9, 12). In this study, we observed motion with respiration because the breath was not held. However, we performed multislice CT, and we investigated the images as three-dimensional CT scans. The study sought to investigate the agreement between PET, CT, and HP findings in the measurement of tumor size. Further studies are needed to investigate the agreement between volumetric measurements obtained from CT, PET, and HP findings.

In conclusion, the PET component of PET-CT is useful for delineating the primary tumor volume of NSCLC if there is surrounding collapse or con-

solidation or possible invasion of the mediastinum; otherwise, CT alone with either soft-tissue or lung windows is adequate. We postulate that PET-CT would be useful for tumor measurement only if consolidation or collapse surrounds the primary tumor. According to the results that we obtained in this study, PET imaging can be regarded as an effective imaging method for calculating tumor measurements. To lend support to our findings in this study, we recommend further prospective studies including a greater number of patients.

Acknowledgement

This study was supported by Akdeniz University Scientific Research Projects Unit.

Conflict of interest disclosure

The authors declared no conflicts of interest.

References

1. Jemal A, Siegel R, Ward E, Murray T, Xu J, Thun MJ. Cancer statistics 2007. *CA Cancer J Clin* 2007; 57:43–66. [\[CrossRef\]](#)
2. Rosell R, Felip E, Maestre J, et al. The role of chemotherapy in early non-small-cell lung cancer management. *Lung Cancer* 2001; 34:63–74. [\[CrossRef\]](#)
3. Rami-Porta R, Ball D, Crowley J, et al. International Staging Committee; Cancer Research and Biostatistics; Observers to the Committee; Participating Institutions. The IASLC Lung Cancer Staging Project: proposals for the revision of the T descriptors in the forthcoming (seventh) edition of the TNM classification for lung cancer. *J Thorac Oncol* 2007; 2:593–602. [\[CrossRef\]](#)
4. Janssen-Heijnen ML, Schipper RM, Razenberg PP, Crommelin MA, Coebergh JW. Prevalence of comorbidity in lung cancer patients and its relationship with treatment: a population-based study. *Lung Cancer* 1998; 21:105–113. [\[CrossRef\]](#)

5. Macpherson RE, Higgins GS, Murchison JT, et al. Non-small-cell lung cancer dimensions: CT-pathological correlation and interobserver variation. *Br J Radiol* 2009; 82:421–425. [\[CrossRef\]](#)
6. Rege SD, Hoh CK, Glaspy JA, et al. Imaging of pulmonary mass lesions with whole-body positron emission tomography and fluorodeoxyglucose. *Cancer* 1993; 72:82–90. [\[CrossRef\]](#)
7. Nolop KB, Rhodes CG, Brudin LH, et al. Glucose utilization in vivo by human pulmonary neoplasms. *Cancer* 1987; 60:2682–2689. [\[CrossRef\]](#)
8. Kelly RF, Tran T, Holmstrom A, Murar J, Seguro RJ Jr. Accuracy and cost-effectiveness of 18F-2-fluoro-deoxy-D-glucose-positron emission tomography scan in potentially resectable non-small cell lung cancer. *Chest* 2004; 125:1413–1423. [\[CrossRef\]](#)
9. Kanzaki R, Higashiyama M, Maeda J, et al. Clinical value of F18-fluorodeoxyglucose positron emission tomography-computed tomography in patients with non-small cell lung cancer after potentially curative surgery: experience with 241 patients. *Interact Cardio Vasc Thorac Surg* 2010; 10:1009–1014. [\[CrossRef\]](#)
10. Hicks RJ, Kalff V, MacManus MP, et al. 18F-FDG PET provides high-impact and powerful prognostic stratification in staging newly diagnosed non-small cell lung cancer. *J Nucl Med* 2001; 42:1596–1604.
11. Rohren EM, Turkington TG, Coleman RE. Clinical applications of PET in oncology. *Radiology* 2004; 231:305–332. [\[CrossRef\]](#)
12. MacManus M, Nestle U, Rosenzweig KE, et al. Use of PET and PET/CT for radiation therapy planning: IAEA expert report 2006–2007. *Radiother Oncol* 2009; 91:85–94. [\[CrossRef\]](#)
13. Chiti A, Kirienko M, Gregoire V. Clinical use of PET-CT data for radiotherapy planning: what are we looking for? *Radiother Oncol* 2010; 96:277–279. [\[CrossRef\]](#)
14. van Baardwijk A, Bosmans G, Boersma L, et al. PET-CT-based auto-contouring in non-small-cell lung cancer correlates with pathology and reduces interobserver variability in the delineation of the primary tumor and involved nodal volumes. *Int J Radiat Biol Phys* 2007; 68:771–778. [\[CrossRef\]](#)

15. Hatt M, Rest CC, Baardwijk AV, Lambin P, Pradier O, Visvikis D. Impact of tumor size and tracer uptake heterogeneity in 18F-FDG PET and CT non-small cell lung cancer tumor delineation. *J Nucl Med* 2011; 52:1690–1697. [\[CrossRef\]](#)
16. Yu HM, Liu YF, Hou M, Liu J, Li XN, Yu JM. Evaluation of gross tumor size using CT, 18F-FDG PET, integrated 18F-FDG PET/CT and pathological analysis in non-small cell lung cancer. *Eur J Radiol* 2009; 72:104–113. [\[CrossRef\]](#)
17. Nestle U, Kremp S, Schaefer-Schuler A, et al. Comparison of different methods for delineation of 18F-FDG PET-positive tissue for target volume definition in radiotherapy of patients with non-small cell lung cancer. *J Nucl Med* 2005; 46:1342–1348.
18. Pawaroo D, Cummings NM, Musonda P, Rintoul RC, Rassl D, Beadsmoore C. Non-small cell lung carcinoma: accuracy of PET/CT in determining the size of T1 and T2 primary tumors. *AJR Am J Roentgenol* 2011; 196:1176–1181. [\[CrossRef\]](#)
19. Boellaard R, O'Doherty MJ, Weber WA, et al. FDG PET and PET/CT: EANM procedure guidelines for tumour PET imaging: version 1.0. *Eur J Nucl Med Mol Imaging* 2009; 37:181–200. [\[CrossRef\]](#)
20. Bland JM, Altman DG. Statistical methods for assessing agreement between two methods of clinical measurement. *Lancet* 1986; 1:307–310. [\[CrossRef\]](#)
21. MacManus MP, Wada M, Matthews JP, Ball DL. Characteristics of 49 patients who survived for 5 years following radical radiation therapy for non-small cell lung cancer: the potential for cure. *Int J Radiat Oncol Biol Phys* 2000; 46:63–69. [\[CrossRef\]](#)
22. McCloud TC, Bourgooin PM, Greenberg RW, et al. Bronchogenic carcinoma: analysis of staging in the mediastinum with CT by correlative lymph node mapping and sampling. *Radiology* 1992; 182:319–323.
23. Webb WR, Gatsonis C, Zerhouni EA, et al. CT and MR imaging in staging non-small cell bronchogenic carcinoma: report of the Radiologic Diagnostic Oncology Group. *Radiology* 1991; 178:705–713.
24. Gupta NC, Tamim WJ, Graeber GG, Bishop HA, Hobbs GR. Mediastinal lymph node sampling following positron emission tomography with fluorodeoxyglucose imaging in lung cancer staging. *Chest* 2001; 120:521–527. [\[CrossRef\]](#)
25. Steinert HC, Hauser M, Allemann F, et al. Non-small cell lung cancer: nodal staging with FDG PET versus CT with correlative lymph node sampling. *Radiology* 1997; 202:441–446.
26. Chan R, He Y, Haque A, Zwischenberger J. Computed tomographic-pathologic correlation of gross tumor volume and clinical target volume in non-small cell lung cancer. *Arch Pathol Lab Med* 2001; 125:1469–1472.
27. Graziano SL. Non-small cell lung cancer: clinical value of new biological predictors. *Lung Cancer* 1997; 17:37–58. [\[CrossRef\]](#)
28. Biehl KJ, Kong F, Dehdashti F, et al. 18F-FDG PET definition of gross tumour volume for radiotherapy of non-small-cell lung cancer: is a single standardised uptake value threshold appropriate? *J Nucl Med* 2006; 47:1808–1812.
29. Hong R, Halama J, Bova D, Sethi A, Emami B. Correlation of PET standard uptake value and CT window-level thresholds for target delineation in CT-based radiation treatment planning. *Int J Radiat Oncol Biol Phys* 2007; 67:720–726. [\[CrossRef\]](#)
30. Lee SM, Goo JM, Park CM, Lee HJ, Im JG. A new classification of adenocarcinoma: what the radiologists need to know. *Diagn Intern Radiol* 2012; 18:519–526.
31. Higashi K, Ueda Y, Seki H, et al. Fluorine-18-FDG PET imaging is negative in bronchoalveolar lung carcinoma. *J Nucl Med* 1998; 39:1016–1020.
32. Heikkila L, Mattila P, Harjula A, Suomalainen RJ, Mattila S. Tumour growth rate and its relationship to prognosis in bronchiolo-alveolar and pulmonary adenocarcinoma. *Ann Chir Gynaecol* 1985; 74:210–214.
33. Hsu PK, Huang HC, Hsieh CC, et al. Effect of formalin fixation on tumor size determination in stage I non-small cell lung cancer. *Ann Thorac Surg* 2007; 84:1825–1829. [\[CrossRef\]](#)
34. Brianzoni E, Rossi G, Ancidei S, et al. Radiotherapy planning: PET/CT scanner performances in the definition of gross tumour volume and clinical target volume. *Eur J Nucl Med Mol Imaging* 2005; 32:1392–1399. [\[CrossRef\]](#)
35. Therasse P, Arbuck SG, Eisenhauer EA, et al. New guidelines to evaluate the response to treatment in solid tumors: European Organization for Research and Treatment of Cancer, National Cancer Institute of the United States, National Cancer Institute of Canada. *J Natl Cancer Inst* 2000; 92:205–216. [\[CrossRef\]](#)